On the Radiation Chemical Kinetics of the Precursor to the Hydrated Electron

Simon M. Pimblott* and Jay A. LaVerne

Radiation Laboratory, University of Notre Dame, Notre Dame, Indiana 46556

Received: December 11, 1997; In Final Form: February 25, 1998

Comparisons of the predictions of stochastic diffusion kinetic calculations using electron track structures with experimental scavenger data show that the precursor to the hydrated electron, e_{pre}^-, plays a role in determining the total yield of electrons scavenged in a number of systems. The significance of e_{pre}^- scavenging on yields depends on the scavenger of interest and on the rate coefficient of the scavenger's reaction with the hydrated electron, e_{aq}^-. For Cd^{2+}, where the reaction ($e_{aq}^- + Cd^{2+}$) is fast, the consequences of e_{pre}^- scavenging are experimentally not apparent, for NO_3^-, a less efficient e_{aq}^- scavenger, the effects of e_{pre}^- reaction are apparent in concentrated solutions, and for SeO_4^{2-}, an inefficient e_{aq}^- scavenger, e_{pre}^- scavenging is obvious even in dilute solution.

1. Introduction

The contribution of the precursor to the hydrated electron, henceforth denoted e_{pre}^-, to the radiation chemistry of water and aqueous solutions has been a topic of interest for some time.[1−4] A great deal of information is known about the hydrated electron, e_{aq}^-, and about its chemistry.[5] However, in contrast to e_{aq}^-, very little is known about e_{pre}^- and its chemistry.[4]

The decay kinetics of e_{aq}^- in the electron pulse radiolysis of deaerated water has been observed by direct absorption spectroscopy over the *3*0 ps to microsecond range.[6−10] There is a reduction in the yield of e_{aq}^- from 4.8 at 30 ps to 2.6 at 1 μs,[11] primarily due to the reactions of e_{aq}^- with H_{aq}^+ and OH.[12] (Radiation chemical yields, *G*-values, are given in units of molecules/100 eV.) In addition, extensive complementary studies have documented the effects of added solutes.[13−16] The yield of e_{aq}^- scavenged by the various solutes rises from 2.5 to >4.4 as the scavenging capacity of the solution is increased from 10^5 to 10^9 s^{-1}.[17] Further studies have measured the yield of molecular hydrogen, H_2. Hydrogen is predominantly formed by the reactions $e_{aq}^- + e_{aq}^- \rightarrow H_2 + 2\ OH^-$ and $e_{aq}^- + H \rightarrow H_2 + OH^-$. [12] Over the scavenging capacity range of 10^5−10^9 s^{-1}, the yield of H_2 drops from 0.45 to ∼0.2.[18] No published studies have clearly addressed the effects of scavenging e_{pre}^- on the yields of e_{aq}^- and of H_2.

Recent femtosecond pulsed laser experiments have shown that e_{pre}^- is short-lived[19]

$$e_{qf}^- \xrightarrow{110\ fs} e_{pre}^- \xrightarrow{240\ fs} e_{aq}^-$$

having a lifetime, τ_{pre}, on the order of 240 fs. Because of the short lifetime of e_{pre}^-, direct observation is difficult. In addition, distinguishing between the reactions of e_{pre}^- and e_{aq}^- with solutes is not straightforward. Nevertheless, e_{pre}^- is believed to be significant in determining the observed radiation chemistry of concentrated solutions of (some) electron scavengers.[4,20]

The yield of e_{aq}^- at short (∼30 ps) times in scavenger solutions has been measured relative to that in neat water by Hunt and co-workers[21,22] and by Jonah et al.[4] Both groups found that the fraction of e_{aq}^- surviving at ∼30 ps is a function of scavenger concentration, [S], and is described by the empirical equation

$$f = \exp(-[S]/C_{37}) \quad (1)$$

with the parameter C_{37} being dependent on the scavenger. In the scavenger systems studied by Lam and Hunt, C_{37} tracked the inverse of the high concentration rate coefficient of the scavenger for e_{aq}^- (with the exception of H_{aq}^+). However, Jonah et al. [4] found several scavengers where C_{37} was not proportional to the rate coefficient. The additional decay in the yield of e_{aq}^- was attributed to the scavenging of a precursor to e_{aq}^-, i.e., to e_{pre}^-. Alternative explanations using a time-dependent rate coefficient for the scavenging of e_{aq}^- [23] or the instantaneous scavenging of e_{aq}^- [24] have also been postulated.

The short-time chemistry in electron radiolysis is characteristic of the competition between the diffusive relaxation of the spatially nonhomogeneous distribution of reactants produced by the radiation and their encounter-limited reaction.[25] The observed kinetics provide the only direct access to the physical and the physicochemical processes; however, to extract useful information about these processes, an accessible model for the chemistry is necessary. Clearly, it is necessary to elucidate the significance of e_{pre}^- in determining the observed outcome. This study describes an analysis of the contribution of e_{pre}^- to the radiation chemistry of water and of several (concentrated) scavenger systems. A diffusion-kinetic methodology is used to examine the scavenging of e_{aq}^- and to derive parameters appropriate for modeling the energetic electron radiolysis of water. Track structure and stochastic diffusion-kinetic simulations are then used in conjunction with the available experimental data to elucidate, and to quantify, the ultimate importance of e_{pre}^- chemistry in radiation chemical kinetics.

2. Methodology

2.1. Fast Scavenging of Electrons. It should be noted that the calculations presented here do not take into account the wave nature of the electron but employ a classical description. While a classical treatment of the properties of e_{pre}^- is not entirely satisfactory, this approximation is unlikely to affect the validity of the discussion of its diffusion-limited kinetics. The classical treatment used here faithfully reproduces the experimental relationship given by eq 1.

S1089-5639(98)00496-4 CCC: $15.00
Published on Web 04/08/1998

The measurements of Hunt and co-workers were made on the 30-ps time scale and those of Jonah et al. were performed on the 50-ps time scale. This experimental time scale is short compared to that usually considered in radiation chemistry; very little chemistry occurs at subnanosecond times.[11,26] To a first approximation, the observed decay in the yield of e_{aq}^- might be attributed to two components, the "instantaneous" scavenging of e_{pre}^- at very short times and the subsequent time-dependent reaction of e_{aq}^- with scavenger.

The scavenging of e_{pre}^- must take place on a subpicosecond time scale as the lifetime of e_{pre}^- in neat water is only of the order 240 fs. Two models for the scavenging kinetics are suggested: a static process in which reaction is by initial overlap or a dynamic process with the scavenging reaction in competition with hydration. If the scavenging of e_{pre}^- is assumed to be static, then the probability of reaction, W, is the probability that an e_{pre}^- overlaps a scavenger. The probability of a scavenger being within a sphere of radius R_{pre} is given by a Poisson distribution; consequently, the probability of static scavenging by initial overlap is

$$W = 1 - \exp(-4\pi L_A[S]R_{pre}^3/3) \tag{2a}$$

where L_A is Avogadro's number. If the reaction of e_{pre}^- with the scavenger is in dynamic competition with hydration of e_{pre}^-, then pseudo-first-order competition kinetics suggests that the probability of scavenging is

$$W = \tau_{pre}k_{pre}[S]/(\tau_{pre}k_{pre}[S] + 1) \tag{2b}$$

where k_{pre} is the rate coefficient for the scavenging reaction (e_{pre}^- + S). In both models, the probability of e_{pre}^- being hydrated to give e_{aq}^- is the complement of W.

The time-dependent survival probability of an isolated e_{aq}^- in a solution of scavenger is given by the diffusion reaction equation

$$d\Omega/dt = -k(t)[S]\Omega \tag{3a}$$

whose solution is

$$\Omega(t) = \Omega(0)\exp(-[S]\int_0^t k(u)\,du) \tag{3b}$$

Here $\Omega(t)$ is the survival probability at time t, $\Omega(0)$ is the instantaneous survival probability, and $k(t)$ is the time-dependent rate coefficient for the reaction (e_{aq}^- + S).

For a diffusion-controlled reaction, the time-dependent rate coefficient is[27,28]

$$k(t) = k_{obs}(1 + (R_{eff} + r_c)/(\pi D't)^{1/2}) \tag{4}$$

where k_{obs} is the limiting steady-state rate coefficient, R_{eff} is the effective reaction radius, and D' is the relative diffusion coefficient of the scavenger and e_{aq}^-. As reaction occurs on encounter

$$k_{obs} = k_{diff} = 4\pi L_A D' R_{eff} \tag{5}$$

If the scavenger is uncharged, the effective reaction distance and the Smoluchowski encounter distance, R, are equivalent. However, when the scavenger is charged, they are related by

$$R_{eff} = -r_c/(1 - \exp(r_c/R)) \tag{6}$$

where r_c is the distance at which the Coulomb potential energy between two ions of charge q_1 and q_2 equals k_BT, that is, $r_c = q_1q_2/(4\pi\epsilon_0\epsilon_r k_BT)$. It is negative for oppositely charged ions and positive for similarly charged ions.

When reaction between e_{aq}^- and the scavenger is only partially diffusion-controlled, the steady-state rate coefficient, k_{obs}, has two components representing the diffusion controlled encounter of the reactants, k_{diff}, and their activation controlled reaction, k_{act}[29]

$$\frac{1}{k_{obs}} = \frac{1}{k_{diff}} + \frac{1}{k_{act}} \tag{7}$$

and the time-dependent rate coefficient is[30]

$$k(t) = \frac{k_{diff}}{(1+\delta)}\left(1 + \frac{1}{\delta}\exp(\beta^2 t)\,\mathrm{erfc}(\beta\sqrt{t})\right) \tag{8}$$

with $k_{obs} = k_{diff}/(1 + \delta)$, where δ is the ratio k_{diff}/k_{act} and β is $4\pi D'L_A(D')^{1/2}/(k_{obs}\ \delta)$. While the parameters in eq 5 for diffusion-controlled scavenging reactions can be uniquely defined, this is not the case for partially diffusion-controlled reaction. An acceptable estimate for δ (actually R_{eff}) has to be made.[31,32]

The formulations for $k(t)$ described above are for dilute solutions. The effects of ionic strength on the time-dependent rate coefficients for the reaction of ions have been discussed previously.[30] The Coulombic distance scaling of eq 6 is replaced by a scaling appropriate for a screened potential. The scaling

$$R_{eff}^{-1} = \sum_{n=0}^{\infty}\left(\frac{\gamma r_c}{R}\right)^n \frac{E_{n+2}(nR/r_D)}{Rn!} \tag{9}$$

is a sum of exponential integrals, $E_i(x)$,[33] and is straightforward to evaluate as the series rapidly converges.[30] Here r_D is the Debye screening length, and the parameter γ is conventionally taken to be $R/2$. In the limit of low ionic strength eq 9 reduces to eq 6.

The time dependence of the rate coefficient, $k(t)$, can have a significant effect on the survival probability of an e_{aq}^- in concentrated solutions of scavengers with large $R_{eff}/\sqrt{D'}$ such as nitrate. Under steady-state conditions, there is a depletion of solute molecules near e_{aq}^-. However, at short times this condition has not yet been achieved and there is a higher concentration of solute molecules, which is taken into account by a larger, time-dependent rate coefficient. At high concentration, ~0.1−1 M, the time dependence of $k(t)$ increases the amount of hydrated electrons scavenged over what would be expected from a steady-state analysis; however, at the lower concentration, $<10^{-3}$ M, the scavenging reactions take place on a time scale over which $k(t)/k_{obs}$ ~1, and there is no observable effect of the time dependence.

Assuming that the survival probability of the e_{aq}^- is given by eq 3b with $\Omega(0) = 1 - W$, then, for a diffusion-controlled reaction, the scavenging radius for e_{pre}^- is

$$R_{pre} = \{3(C_{37}^{-1} - k_{obs}(t + 2(R_{eff} + r_c)t^{1/2}/(\pi D')^{1/2}))/(4\pi L_A)\}^{1/3} \tag{10a}$$

and the rate coefficient for the (e_{pre}^- + S) reaction is

$$k_{pre} = \frac{\exp((C_{37}^{-1} - k_{obs}(t + 2(R_{eff} + r_c)t^{1/2}/(\pi D')^{1/2}))[S]) - 1}{\tau_{pre}[S]} \quad (11a)$$

For a partially diffusion-controlled reaction of e_{aq}^- with a scavenger

$$R_{pre} = \left(3\left\{C_{37}^{-1} - k_{obs}\left(t + \frac{1-\delta}{\delta\beta^2}(\exp(\beta^2 t)\,\mathrm{erfc}(\beta\sqrt{t}) - 1 + 2\beta\sqrt{t/\pi}\right)\right\}/(4\pi L_A)\right)^{1/3} \quad (10b)$$

and

$$k_{pre} = \left\{\exp\left([S]C_{37}^{-1} - k_{obs}[S]\left(t + \frac{1-\delta}{\delta\beta^2}(\exp(\beta^2 t) \times \mathrm{erfc}(\beta\sqrt{t}) - 1 + 2\beta\sqrt{t/\pi}\right)\right) - 1\right\}/\tau_{pre}[S] \quad (11b)$$

In eqs 10 and 11, t is the time at which the C_{37} value is measured, i.e., ~30 ps. Equations 11 suggest that k_{pre} is dependent on scavenger concentration, which is not aesthetically pleasing. Calculations, however, show that this dependence is small, except at extremely high scavenger concentration, >1 M.

2.2. Simulation of the Electron Radiolysis of Aqueous Solutions. A number of different techniques have been developed for modeling the fast chemistry of the electron radiolysis of water.[12,17,31,34−39] Many recent studies have focused on the use of simulated track structures[40−42] in stochastic modeling of the kinetics using either a random flights[36,37] or an independent reaction times[12,38,39] (IRT) methodology. This type of analysis has the advantage over more conventional deterministic methods in that it correctly incorporates reactants in their actual nonhomogeneous spatial distribution.[43,44] The following calculations are based on the independent reaction times diffusion-kinetic model and make use of simulated 10-keV sections of 1-MeV electron tracks produced using liquid water cross sections.[41,42,45,46]

The tracks are simulated by following the path of the primary electron collision-by-collision until its energy is attenuated from 1 MeV to 990 keV, and paths of the secondary daughter electrons until their energy is attenuated to thermal. The distance between collisions is obtained by sampling from a Poisson distribution with a mean free path, which is dependent on the electron energy. The nature of each collision is determined by the relative cross sections for the ionization, excitation, vibration, and elastic processes. The energy loss in inelastic collisions is calculated from the differential inelastic cross section in energy, and any trajectory deviations are evaluated either from the kinematics (inelastic events) or by sampling from the differential elastic cross section in angle (elastic events). The energy of every electron is followed until a suitable predefined cutoff is reached. In the following calculations, secondary electron trajectories are simulated to a final energy of 25 eV, and then an analytic method, derived from techniques presented in ref 47, is used to determine the probability of further terminal low-energy ionization and excitation events. This simulation methodology and the cross sections employed are described in detail in ref 12.

The diffusion kinetic modeling using the IRT method begins from the initial spatial distribution of the reactants given by the track structure simulation. The relative separations of the particles are determined and then used to evaluate which reactants are in a reactive configuration. Reaction times are generated for those pairs not overlapping. The minimum of the ensemble of times represents the reaction time of the first pair. After this pair has reacted, new reaction times are generated for the reactive products using the "diffusion approach" of Clifford et al.[48] and the simulation proceeds in the same manner until a predefined cutoff time is reached. The simulation of many different tracks (usually >100) is necessary to obtain adequately averaged chemistry. The IRT methodology has been described in detail,[48−50] as has its application to electron track structures.[12,38,39]

TABLE 1: Reaction Scheme for the Short-Time Radiolysis of Water

reaction	$k/10^{10}$ M^{-1} s^{-1}	R_{eff}/nm	R[a]/nm
$e_{pre}^- \rightarrow e_{aq}^-$	7.6	(t = 240 fs)	
$e_{aq}^- + e_{aq}^- \rightarrow H_2 + 2\,OH^-$	0.55	0.16	0.42
$e_{aq}^- + H_{aq}^+ \rightarrow H$	2.3	0.23	0.50
$e_{aq}^- + H \rightarrow H_2 + OH^-$	2.5	0.29	
$e_{aq}^- + OH \rightarrow OH^-$	3.0	0.54	
$e_{aq}^- + H_2O_2 \rightarrow H_2 + 2\,OH^-$	1.1	0.22	
$H_{aq}^+ + OH^- \rightarrow H_2O$	14.3	1.35	0.96
$H + H \rightarrow H_2$	0.78	0.15	
$H + OH \rightarrow H_2O$	2.0	0.27	
$H + H_2O_2 \rightarrow OH + H_2O$	0.009	0.001	
$OH + OH \rightarrow H_2O_2$	0.55	0.26	

[a] Where an R is not given, the reaction is taken to be close to diffusion-controlled and R is the same as R_{eff}.

TABLE 2: Diffusion Coefficients for the Reactants Involved in the Short-Time Radiolysis of Water

reactant	$D/\times 10^{-8}$ m^2 s^{-1}	reactant	$D/\times 10^{-8}$ m^2 s^{-1}
e_{aq}^-	0.45	OH	0.28
H_{aq}^+	0.90	OH^-	0.50
H	0.70	H_2O_2	0.22

The reaction scheme for the radiolysis of water used in the calculations is essentially that due to Schwarz.[34] The reaction radii (R and R_{eff}) and the diffusion coefficients (D) were derived from the compilations of Buxton, Elliot, and co-workers[51,52] in ref 50 and are summarized in Tables 1 and 2. The only exception is the rate coefficient for the solvation of e_{pre}^- to e_{aq}^-, which was assumed to be 7.6×10^{10} M^{-1} s^{-1}, as suggested by the lifetime measurements of Gauduel and co-workers. [19]

Calculations have shown that the simulated kinetics of the first 10-keV sections of 1-MeV tracks are statistically different from the kinetics of the complete tracks, but the differences are smaller that the errors in the available experimental data with which the calculations can be compared.[53]

3 Results and Analysis

The kinetics of e_{pre}^- and of e_{aq}^- predicted for the energetic electron radiolysis of neat water are shown in Figure 1. The ionization yield predicted by the track structure simulation is 4.9. At 1 ps the yield of e_{pre}^- is about 0.1, while that of e_{aq}^- is 4.8. The rapid solvation of e_{pre}^-, measured in femtosecond laser experiments,[54,55] occurs before any significant chemistry with other spur reactants has occurred. Detailed examination of the simulated kinetics shows that e_{pre}^- does not participate in the intratrack reactions of pure water resulting in observable chemistry. The experimental decay kinetics of e_{aq}^- obtained from direct absorption measurements[6−10,26] and from the inverse Laplace transform analysis of scavenger data are also included in the figure.[11,17] There is good agreement between calculation and experiment over the whole time range. The e_{aq}^- yield on

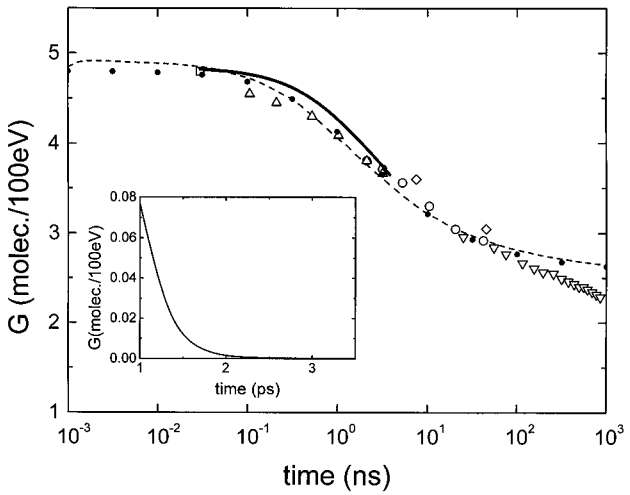

Figure 1. Time-dependent kinetics of the electron radiolysis of deaerated water. Yields of e_{aq}^- measured by direct spectroscopic absorption are ref 6 (◇), ref 7 (▽), ref 9 stroboscopic detection method (△), ref 9 CW laser/photodiode detection method (○), ref 10 (□), ref 26 (bold line). The time dependence of e_{aq}^- obtained by the inverse Laplace transform of scavenger data is given by the dotted line.[11] The predictions of stochastic diffusion-kinetic calculations using electron track structures are shown as the solid line for e_{pre}^- and the dashed line for e_{aq}^-.

the picosecond time scale is ∼4.9, and this drops to ∼2.6 by 1 ms, while the majority of the intratrack reaction takes place on the 0.1−10 ns time scale.

Figure 1 demonstrates that e_{pre}^- is not significantly involved in the observed intratrack radiation chemistry of pure water; however, in concentrated aqueous solutions scavenging reactions may take place at early times. Two types of scavenging reaction may contribute to the observed chemistry, scavenging of e_{pre}^- and of e_{aq}^-. The scavenging radii for a number of e_{aq}^- scavengers calculated using the experimental C_{37} values of Jonah et al.[4] in eq 10a are listed in Table 3. The table also includes effective radii of the neutral molecules[56] and the hydrated ions,[57] and the effective reaction distances and the encounter distances for (e_{aq}^- + S). The R_{pre} of H_2O_2 is ∼0, while the R_{pre}'s of acetone and the hydrated anions are considerably larger than the corresponding effective radii, effective reaction distances, and encounter distances. For the cations, Cu^{2+} and Cd^{2+}, the scavenging reactions cannot be treated as diffusion-controlled since $R_{eff} < r_c$. When reaction is only partially diffusion-controlled it is necessary to make "an educated guess" for the encounter radius, which then gives the ratio $\delta = k_{diff}/k_{act}$.

The sizes of the R_{pre} obtained using eq 10a suggest that e_{pre}^- may play a role in determining the chemistry of a number of scavenger solutions. To determine this effect, it is necessary to consider the particular scavenger of interest as the C_{37} values do not correlate with the steady-state rate coefficients for the e_{aq}^- scavenging reactions. Of the scavengers considered only one, H_2O_2, has $R_{pre} \sim 0$ and does not appear to scavenge e_{pre}^-.

3.1. Nitrate. The experimental value of C_{37} for the nitrate is 0.42 M. Nitrate is a very efficient scavenger of e_{aq}^- with a scavenging rate coefficient of 9.7×10^9 M^{-1} s^{-1}. Figure 2a considers the effect of nitrate concentration on the survival probability of e_{aq}^-. The curve for the C_{37} values of Jonah et al. [4] shows significant scavenging (at 50 ps) at high scavenging capacities and cannot be explained in terms of scavenging of hydrated electrons; the curve differs significantly from the predictions of eq 3b with $\Omega(0) = 1$. The quantity $\Omega(t)/\Omega(0)$ is equivalent to the time-dependent survival probability (at 50 ps) if there is no instantaneous scavenging of e_{pre}^- or e_{aq}^-. For the $\Omega(t)/\Omega(0)$ curve to match the experimental data for NO_3^-, a time of 100 ps, not 50 ps, is required. A time scale in error by a factor of 2 is not experimentally justifiable.

The fraction of e_{pre}^- surviving instantaneous scavenging is obtained by dividing eq 1 by eq 3b (with $\Omega(0) = 1$) and is included in the figure. In nitrate solutions, the surviving fraction of electrons at 50 ps is determined by both the scavenging of e_{pre}^- and the time-dependent scavenging of e_{aq}^-, with the two components being of similar significance. According to eq 10, the C_{37} value of 0.42 suggests an e_{pre}^- scavenging radius of 0.74 nm for nitrate. This radius for the e_{pre}^- scavenging reaction is about twice the effective radius of the hydrated NO_3^- anion and twice the Smoluchowski encounter radius for the scavenging of e_{aq}^- by NO_3^-, 0.34 and 0.46 nm, respectively.

The radiolysis of NO_3^- solution produces NO_2^- as an observable product; however, the chemistry of the system is not straightforward,[58] and the measured yields of NO_2^- cannot be related to primary radical yields.[59] The production of NO_2^- occurs via a multistep mechanism involving the intermediates NO_3^{2-} and NO_2, as follows

$$e_{aq}^- + NO_3^- \rightarrow NO_3^{2-} \qquad k = 9.7 \times 10^9\ M^{-1}\ s^{-1}$$

$$NO_3^{2-} + H_2O \rightarrow NO_2 + 2\ OH^- \qquad k \sim 1 \times 10^5\ M^{-1}\ s^{-1}$$

$$NO_2 + NO_2 + H_2O \rightarrow NO_2^- + NO_3^- + 2\ H_{aq}^+ \qquad k \sim 4 \times 10^8\ M^{-1}\ s^{-1}$$

In addition to the complex reaction mechanism, the stoichiometry of the conversion of e_{aq}^- to NO_2^- via NO_3^{2-} is not assured.[59] In fact, Barker et al. have shown that there is a deficit in the yield of NO_2^- of about 15%.[59] Experimental data describing the effect of nitrate on the yield of NO_2^- is shown in Figure 3. Also included in the figure are the predictions of stochastic simulations using energetic electron track structures. The scavenging radius for the ($e_{pre}^- + NO_3^-$) reaction was taken to be 0.74 nm (cf. Table 3), and the ($e_{aq}^- + NO_3^-$) reaction was assumed to be diffusion-controlled and governed by a time-dependent rate coefficient.[31] The calculated yield of NO_2^- is in good agreement with the experimental data of Hyder[60] once the correction of Barker et al. is incorporated.

In solutions of OH scavengers such as CH_3OH, C_2H_5OH, or HCO_2^-, NO_2^- is primarily formed by reaction of NO_2 with an organic radical, e.g.

$$OH + HCO_2^- \rightarrow CO_2^- + H_2O \qquad k = 3.2 \times 10^9\ M^{-1}\ s^{-1}$$

$$NO_2 + CO_2^- \rightarrow NO_2^- + CO_2 \qquad k = 5.9 \times 10^9\ M^{-1}\ s^{-1}$$

The bimolecular reaction, $NO_2 + NO_2$, still provides an alternate route especially at high NO_3^- concentrations. Experimental[61] and simulated yields of NO_2^- for NO_3^-/HCO_2^- solutions are also compared in Figure 3. With the correction of Barker et al., the two sets of data agree well. In addition, detailed examination of the simulated kinetics reveals that NO_2^- is formed almost completely by reaction of NO_2 with organic radicals. For 1 M solution, the bimolecular contribution is only 6% of the NO_2^- yield.

3.2. Selenate. The experimental value of C_{37} for the selenate is the same as that for the nitrate, 0.42 M, even though the scavenging rate coefficients of the anions for e_{aq}^- are very different, 1.1 and 9.7×10^9 M^{-1} s^{-1}, respectively. The two scavengers have similar reactivity with e_{pre}^-; however, NO_3^- is a much more efficient scavenger of e_{aq}^- than selenate. Figure

TABLE 3: Reaction Radii for Common Electron Scavengers

S	C_{37}/M	$k_{obs}/10^{10}$ M^{-1} s^{-1}	$D/10^{-9}$ m^2 s^{-1}	effective radius/nm	R_{eff}/nm	*R*/nm	R_{pre}/nm (e_{aq}^- rxn)	$k_{pre}{}^e/10^{12}$ M^{-1} s^{-1}
acetone	1.4	0.65	1.3	0.31[a]	0.15	0.15	0.48	0.84
H_2O_2	1.44	1.1	2.2	0.21[a]	0.22	0.22	0	0
NO_2^-	1.6	0.41	1.4		0.09	0.32	0.32	0.35
NO_3^-	0.42	0.97	2.0	0.34[b]	0.20	0.46	0.74	4.5
SeO_4^{2-}	0.42	0.11	1.0	0.38[b]	0.03	0.35	0.95	10.0
Cu^{2+}	0.9	3.9	0.7	0.42[b]	0.99	pdc[c]		
Cd^{2+}	0.38	4.8	0.7	0.43[b]	1.22	pdc[c]	(0.63)[d]	(2.8)[d]

[a] Derived from the experimental molar volume.[56] [b] Taken from ref 57. [c] pdc: partially diffusion-controlled reaction for which *R*, δ, and R_{pre} are not uniquely defined. [d] Calculated assuming $R = 2.0$ nm. [e] Calculated for 0.1 M solution.

2b considers the effect of selenate concentration on the survival probability of e_{aq}^-. The curve for the C_{37} value of Jonah et al.[4] shows significant scavenging at 50 ps at high e_{aq}^- scavenging capacities and cannot be explained only in terms of scavenging of hydrated electrons. For the curve of $\Omega(t)/\Omega(0)$ to match the experimental data for selenate, a time of 1 ns is required, which is in error by a factor of 20. In contrast to nitrate solutions, the yield of e_{aq}^- in selenate solutions is determined predominantly by the fraction of e_{pre}^- scavenged. The scavenging of e_{aq}^- plays only a minor role. According to eq 10a, the C_{37} value of 0.42 suggests a scavenging radius of 0.95 nm for selenate. This radius is almost the same as would be predicted if no scavenging of e_{aq}^- took place (0.98 nm) and is considerably larger than the Smoluchowski encounter radius for the scavenging of e_{aq}^-, 0.35 nm. Significantly, the encounter radius is very similar to the effective radius of the hydrated selenate ion, 0.38 nm.

3.3. Cadmium(II). The reaction of e_{aq}^- with Cd^{2+}, unlike those with NO_3^- and SeO_4^{2-}, is not fully diffusion-controlled. The C_{37} value for Cd^{2+} is 0.38 M, slightly smaller than the corresponding values for NO_3^- and for SeO_4^{2-}. However, this difference is much smaller (~10%) than the differences in the scavenging rate coefficients for e_{aq}^- (a factor of ~5 for NO_3^- and ~50 for SeO_4^{2-}). Experimentally, Cd^{2+}, NO_3^-, and SeO_4^{2-} cause similar decays of e_{aq}^- on the 50-ps time scale, but Cd^{2+} is much more reactive toward e_{aq}^-. This fact suggests that the scavenging of e_{pre}^- by Cd^{2+} is chemically less dominant than the scavenging of e_{pre}^- by NO_3^- or by SeO_4^{2-}.

The effect of Cd^{2+} concentration on the survival probability of an e_{aq}^- at 50 ps is considered in Figure 2. Since the reaction ($e_{aq}^- + Cd^{2+}$) is only partially diffusion-controlled ($R_{eff} < r_c$), the Smoluchowski encounter radius is not uniquely defined by the steady-state rate coefficient,[27] and a suitable estimate is necessary. As the value of *R* (and therefore of δ) is varied, the calculated surviving fraction of e_{aq}^- at 50 ps changes. Curves are shown for *R* equal to 0.5, 1.0, 1.5, and 2.0 nm. An encounter radius smaller than 1.5 nm gives more reaction than is observed experimentally by Jonah et al., [4] even without including reaction of e_{pre}^- with the Cd^{2+} ion. At $R = 1.5$ nm, the experimental decay is reproduced. This value of *R* is about three times the effective radius of the hydrated Cd^{2+} ion. Furthermore, the implied value of the ratio δ is 0.9, compared to 0.2 when the encounter radius is equal to the radius of the hydrated ion.[52] Clearly, the reaction of e_{aq}^- with Cd^{2+} is not diffusion-limited. The scavenging radius of Cd^{2+} for e_{pre}^- is very sensitive to *R* for *R* less than about ~1.8 nm but is insensitive to *R* for larger values. In the following simulations, *R* was assumed to be 2.0 nm, giving δ and R_{pre} of 1.28 and 0.64 nm, respectively. (In fact, the results of the radiation chemical kinetic simulations are fairly insensitive to the exact value of *R* selected.) The effect of Cd^{2+} concentration on the probability of scavenging e_{pre}^- is shown in Figure 2c. Using the parameters suggested, the majority of the observed electron scavenging at 50 ps is via the ($e_{pre}^- + Cd^{2+}$) reaction.

A series of stochastic diffusion kinetics calculations using simulated electron track structures have been performed for the radiation chemical kinetics of Cd^{2+} solutions. The time dependence of the yields of e_{pre}^-, e_{aq}^-, Cd^+, and Cd_2^{2+} in 1 M Cd^{2+} are shown in Figure 4. On the picosecond time scale, e_{pre}^- is converted into e_{aq}^- and Cd^+: the yields at 1ps are ~ 0.02, 1.5, and 3.5, respectively. By 0.1 ns, all the e_{aq}^- has been scavenged by Cd^{2+} giving Cd^+, which then decays slowly,[62,63]

$$Cd^+ + Cd^+ \rightarrow Cd_2^{2+} (\Leftrightarrow Cd^0 + Cd^{2+})$$

$$2k \sim (3-8) \times 10^9\ M^{-1}\ s^{-1}$$

Included in the figure are the experimental measurements of Wolff et al.[3] for the yield of Cd^+ at 30 ps and for the yield of Cd^+ equivalents at 30 ps, at 6 ns, and at 100 ns. In their estimation of the yield of Cd^+ equivalents at 30 ps, Wolff et al. assumed the yield of e_{aq}^- in deaerated water is 4.0 at 30 ps[64] and 2.8 at 100 ns. The accepted values are now 4.8 at 30 ps and 2.7 at 100 ns.[10,11] Consequently, the expression for the yield of Cd^+ equivalents at 30 ps is modified to $G(Cd^+) = 1.0G(e_{aq}^-)$ and that for the yield of Cd^+ at 100 ns becomes $G(Cd^+) = 1.50G(e_{aq}^-)$. (No modification of the 6 ns integrated yields is necessary.) An experimental estimate for the yield of e_{aq}^- at 30 ps is also included in Figure 4. This value was obtained by renormalizing the e_{aq}^- data of Wolff et al. to take account of the fact that the yield of e_{aq}^- in deaerated solution at 30 ps is 4.8 and not 4.0 as assumed in their analysis. The agreement between the calculated kinetics and the experimental data is excellent.

The effect of Cd^{2+} concentration on the yields of Cd^+ and of e_{aq}^- is considered in Figures 5 and 6. Figure 5 shows the concentration dependence of Cd^+ and e_{aq}^- at 30 ps. The calculated Cd^+ yields at 30 ps are in good agreement with the stroboscopic pulse radiolysis measurements of Figure 6 in ref 3. In addition, the calculated yields of e_{aq}^- at 30 ps match the experimental data corrected to the accepted value for deaerated water, 4.8[10,11] rather than 4.0. Figure 6 considers yields of Cd^+ at longer times. Three sets of calculations are shown: the Cd^+ yield at 6 ns and at 100 ns and the maximum Cd^+ yield attained. Yields measured by conventional pulse radiolysis at ~100 ns[3,14] compare favorably with predicted yields at 100 ns, and the 6-ns yields obtained by Wolff et al. using stroboscopic pulse radiolysis are also accurately reproduced by calculation.

3.4. Prediction of the Yield of Electrons Scavenged. Scavenger systems are commonly used to estimate the yield of e_{aq}^- in the radiolysis of water. Consequently, understanding the effects of scavenging e_{pre}^- on radiolytic yields is important. The effect of scavenger concentration on the yield of the reaction of electrons with scavenger is considered in Figure 7. The figure compares calculations for a generic e_{aq}^- scavenger (e.g., MeCl

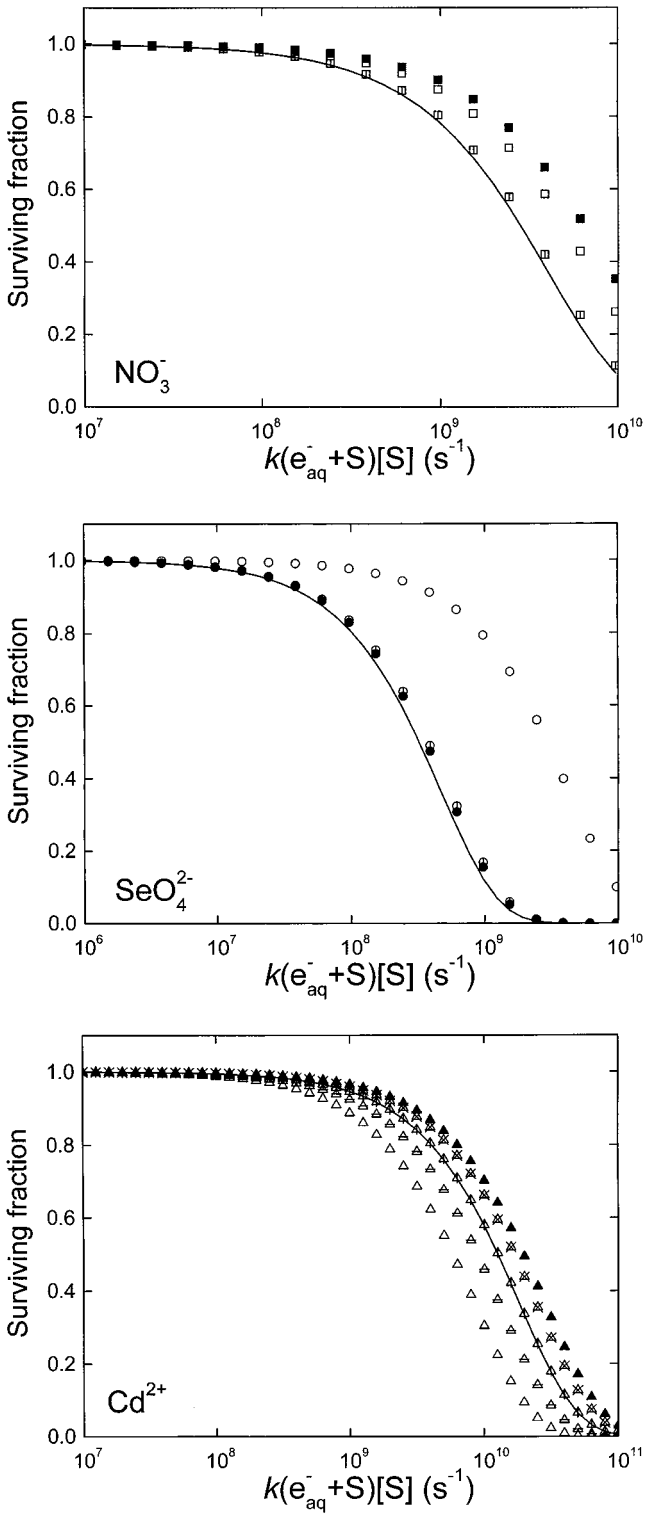

Figure 2. Surviving fraction of e_{aq}^- at 50 ps. The solid lines are calculated using the experimental C_{37} values of Jonah et al.[4] The open points are calculations of $\Omega(t)/\Omega(0)$ for e_{aq}^- and the solid points are estimates for $\Omega(0)$ calculated from the experimental values and from the curves for $\Omega(50\text{ ps})/\Omega(0)$. (a, top) NO_3^- (□) $t = 50$ ps, (□ with a vertical bar) $t = 0.1$ ns; (b, middle) SeO_4^{2-} (○) $t = 50$ ps, (○ with a vertical bar) $t = 1.0$ ns; (c, bottom) Cd^{2+} (all points for 50 ps) (△) $R = 0.5$ nm, (△ with a horizontal bar) $R = 1.0$ nm, (△ with a vertical bar) $R = 1.5$ nm, (△ with a central ×) $R = 2.0$ nm, (▲) estimate for $\Omega(0)$ assuming $R = 2.00$ nm.

or H_2O_2 that does not react with e_{pre}^-) with experimental scavenger data taken from refs 13, 15, and 16 and with the Laplace transform of the decay kinetics of e_{aq}^- in deaerated

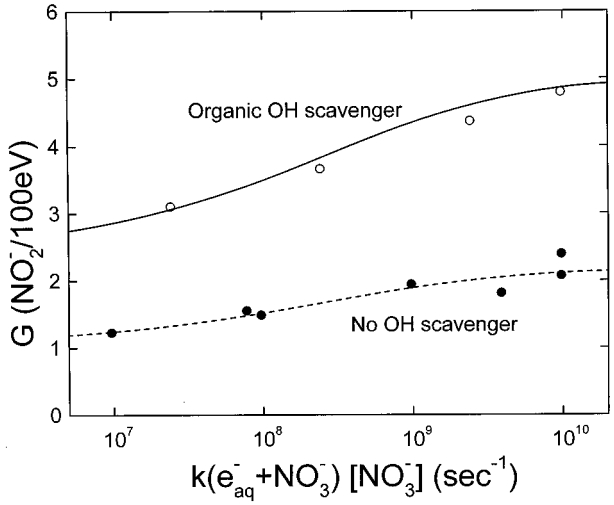

Figure 3. Effect of nitrate concentration on the yield of nitrite in electron radiolysis. The points refer to experimental data, and the lines are the predictions of stochastic diffusion kinetic calculations using electron track structures. Yield of NO_2^- in the presence of formate, (○)[61] and solid line; yield of NO_2^- with no organics present, (●)[60] and dashed line.

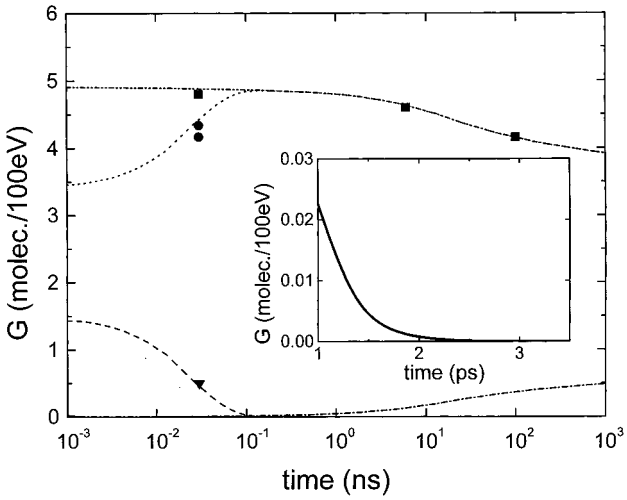

Figure 4. Radiation chemical kinetics of the electron radiolysis of 1 M Cd^{2+} solution. The points refer to experimental data,[3,10] and the lines are the predictions of stochastic diffusion kinetic calculations using electron track structures. e_{pre}^-, solid line; e_{aq}^-, (▼) and dashed line; Cd^+, (●) at 30 ps, (■) at longer times, and dotted line; Cd^+ equivalents, (■) and dot−dot−dashed line; Cd_2^{2+}, dot−dashed line.

water.[11] The agreement between calculation and the data is very good. For scavenging capacities less than 10^9 s^{-1}, the simulated yield (of Cl^- from MeCl solutions) tracks the measured yield. At very high scavenging capacities, there is a small discrepancy between the Laplace transform of the decay kinetics of e_{aq}^- and the simulated yield of e_{aq}^- scavenged, although this difference is probably due to the empirical function used to fit the experimental kinetics.[65]

Calculations for the effect of NO_3^- concentration on the yield of electrons (e_{pre}^- and e_{aq}^-) scavenged are also included in Figure 7. For e_{aq}^- scavenging capacities less than 10^8 s^{-1}, the ($e_{pre}^- + NO_3^-$) reaction does not have an effect on the amount of electrons scavenged. At higher concentrations, $k(e_{aq}^- + S)[S] \sim 10^9$ s^{-1}, the scavenging of e_{pre}^- has a statistically (though probably not experimentally) significant effect on the amount of electrons scavenged. This difference becomes more distinct as the concentration of NO_3^- increases, with the two calculations converging again at an e_{aq}^- scavenging

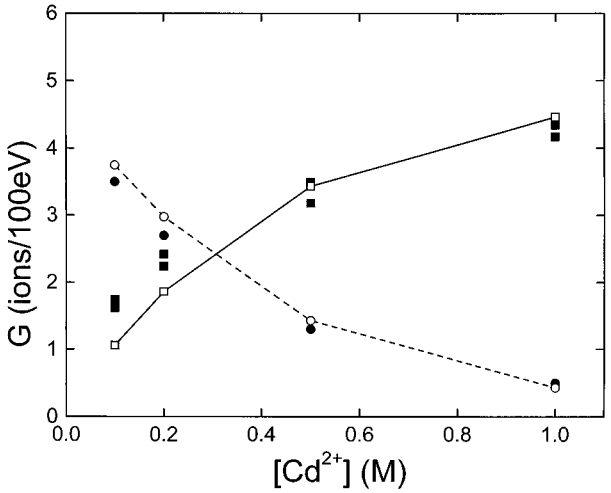

Figure 5. Effect of Cd^{2+} concentration on the yields of Cd^+ and of e_{aq}^- at 30 ps following electron irradiation. The points refer to experimental stroboscopic pulse radiolysis data,[3,10] and the lines are the predictions of stochastic diffusion-kinetic calculations using electron track structures. Cd^+, (■) and solid line with □; e_{aq}^-, (●) and dashed line with ○.

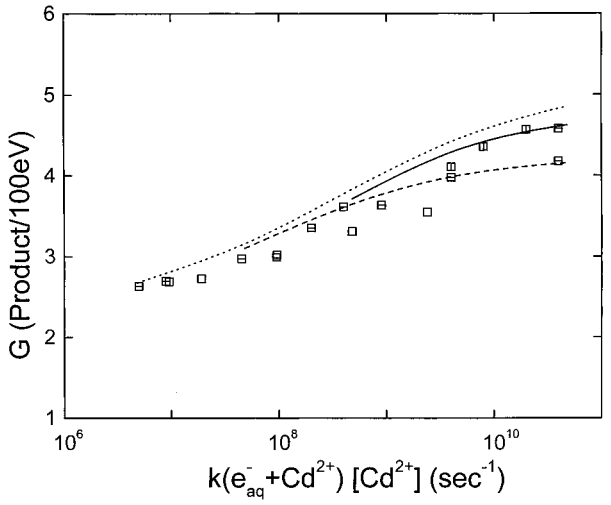

Figure 6. Effect of Cd^{2+} concentration on the yields of Cd^+ at long times. The points refer to experimental data, and the lines are the predictions of stochastic diffusion kinetic calculations using electron track structures. Experiment: conventional pulse radiolysis measurement of Cd^+ (□)[14]; conventional pulse radiolysis measurement of Cd^+ at ~100 ns, □ with a horizontal bar[3]; stroboscopic pulse radiolysis measurement of Cd^+ at ~6 ns, □ with a vertical bar. Calculation: maximum Cd^+ yield (solid line); Cd^+ yield at 6 ns (dashed line); Cd^{2+} yield at 100 ns (dotted line).

capacity of 10^{11} s^{-1}. The experimentally predicted effect of nitrate on the yield of electrons scavenged is included in the figure. Agreement between the calculated yield and the experimental estimate is very good.

The predicted effect of selenate concentration on the amount of electrons scavenged is shown in Figure 7. This curve is shifted considerably from those for the generic e_{aq}^- scavenger and for NO_3^-. The shift reflects the primary role the reaction of e_{pre}^- with SeO_4^{2-} plays in determining the amount of scavenging. Only in very dilute solution is the reaction of e_{aq}^- with SeO_4^{2-} dominant. Unfortunately, experimental data for the yields in the radiolysis of SeO_4^{2-} solutions are not available. The time at which the maximum Cd^+ yield is reached depends on the Cd^{2+} concentration, with the time decreasing as the concentration increases. The calculated maximum Cd^+ yield

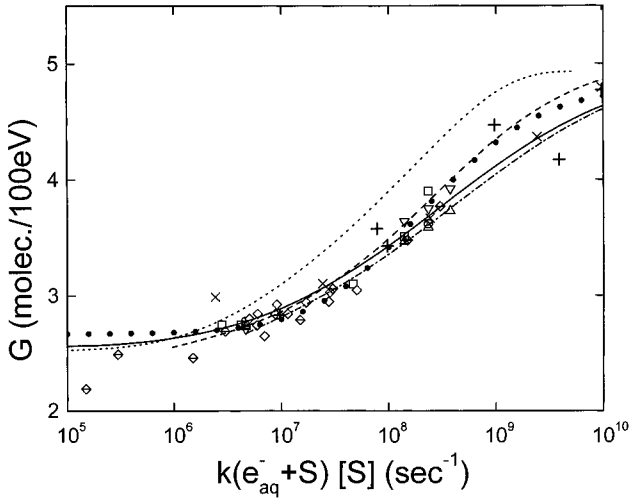

Figure 7. Effect of scavenging capacity for e_{aq}^- on the yield of electrons scavenged. The open points refer to experimental data. Yield of Cl^- from MeCl solutions: ref 13 MeCl (□), MeCl + 10^{-3} M MeOH (○), MeCl + 10^{-2} M MeOH (△), MeCl + 10^{-1} M MeOH (▽); ref 16 MeCl + 10^{-2} M PrOH (◇); ref 60 NO_3^- (+), ref 61 NO_3^- + MeCOMe (×). Yield of NH_3 from glycylglycine solutions: ref 68 glycylglycine (◇ with horizontal slash).). The (●) line is the Laplace transform of the direct absorption data shown in Figure 1.[11] The predictions of stochastic diffusion-kinetic calculations using electron track structures are shown as follows: (solid line) yield of (e_{aq}^- + S) reaction for a generic e_{aq}^- scavenger, (dashed line) total yield of electrons scavenged by NO_3^-, (dotted line) total yield of electrons scavenged by SeO_4^{2-}, (dot−dashed line) maximum yield of Cd^+ in Cd^{2+} solution.

is also included in Figure 7. By coincidence, this curve matches the curve for the generic e_{aq}^- scavenger.

3.5. Yield of e_{pre}^- Scavenging. The data presented in the previous sections have shown that the scavenging of e_{pre}^- can have an observable effect on the yield of products in some scavenger systems. The significance of the effect depends on the relative rate coefficients for the scavenger reactions with e_{pre}^- and e_{aq}^-. The relative importance of these two reactions can be determined by detailed analysis of the stochastic calculations presented. These calculations give insight into chemistry that is difficult to obtain directly from the observed e_{aq}^- kinetics.

The fraction of electrons scavenged before they undergo hydration to e_{aq}^- is considered in Figure 8. For a generic e_{aq}^- scavenger such as MeCl or H_2O_2, this ratio is obviously zero for all $k(e_{aq}^- + S)[S]$. For the three scavengers discussed earlier, the importance of e_{pre}^- scavenging increases in the order Cd^{2+} < NO_3^- < SeO_4^{2-} at low scavenging capacity. A concentration of 1 M scavenges ~90% of the electrons before hydration for SeO_4^{2-} and NO_3^- and ~70% for Cd^{2+}. Despite the significant contribution of the scavenging of e_{pre}^- to the scavenged yield of electrons, the observed chemical outcome is not necessarily different than if no e_{pre}^- scavenging occurred. Comparison of the absolute yield of electrons scavenged in 1 M NO_3^- and in 1 M Cd^{2+} solutions with the predictions for a generic e_{aq}^- scavenger shows very little discrepancy, cf. Figure 7. Only in the case of SeO_4^{2-} is the yield of electrons scavenged significantly different from that expected for a generic e_{aq}^- scavenger. The rate coefficients for the scavenging of e_{pre}^- are large for all the scavengers. The different chemistry reflects the rate coefficients for the (e_{aq}^- + S) reactions, which differ by an order of magnitude.

While the significance of scavenging e_{pre}^- may not be apparent in the yield of electrons scavenged, other radiation chemical observables may be affected. Molecular hydrogen is

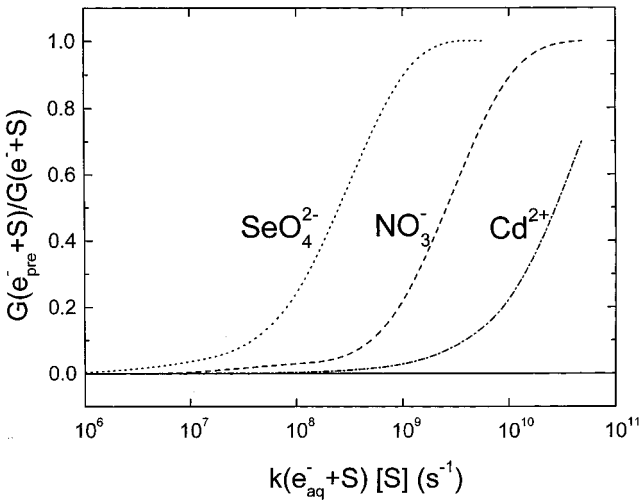

Figure 8. Fraction of electrons scavenged prior to hydration as a function of scavenging capacity for e_{aq}^-. The predictions of stochastic diffusion kinetic calculations using electron track structures are shown as follows: (solid line) generic e_{aq}^- scavenger, (dot−dashed line) Cd^{2+} (dashed line) NO_3^-, and (dotted line) SeO_4^{2-}.

TABLE 4: Effect of e_{pre}^- Scavenging on the Yield of H_2 in NO_3^- Solution

scavenging capacity, $k(e_{aq}^- + S)[S]/s^{-1}$	$G(H_2, NO_3^-$ solution$)/G(H_2, H_2O_2$ solution$)$[a]	
	experiment[18,66]	simulation
10^8	0.97	0.97
10^9	0.87	0.88
10^{10}	0.53	1.0,[b] 0.58[c]

[a] H_2O_2 is assumed to be a generic e_{aq}^- scavenger since $R_{pre} \sim 0$. [b] Calculated assuming the unimolecular H_2 is directly formed. [c] Calculated assuming a scavengable precursor to the unimolecular H_2.

produced by unimolecular (physicochemical) processes and by intratrack reactions involving e_{aq}^- and H. The dominant chemical reactions giving H_2 at neutral pH are $e_{aq}^- + e_{aq}^- \rightarrow H_2 + 2\ OH^-$ and $e_{aq}^- + H \rightarrow H_2 + OH^-$. Both of these reactions have a yield of ∼0.15[12] and will be affected by the scavenging of e_{pre}^- and e_{aq}^-. The ratio of the yield of H_2 produced in NO_3^- solution compared to that of a generic e_{aq}^- scavenger (H_2O_2) solution is given in Table 4. At a scavenging capacity of 10^8 s^{-1} (∼10^{-2} M), the scavenging of e_{pre}^- does not affect the measured yield of H_2, but at 10^9 s^{-1} (∼10^{-1} M) it results in a decrease in the yield of H_2 by an additional 12%. This decrease, predicted by the stochastic simulations, is found in experimental data.[18,66]

It has been suggested that the physicochemical processes leading to the unimolecular production of H_2 involve very low energy electrons.[67] If this is the case, then the H_2 produced in this manner may be scavengable in concentrated solutions of e_{pre}^- scavengers. The track structure simulations employed in ref 12 assumed that the unimolecular H_2 is directly produced. Calculations have been performed incorporating a low-energy electron precursor to unimolecular H_2 that has a lifetime of 110 fs in water (cf. e_{qf}^-). In nitrate solutions, the scavenging of this species does not affect the yield of H_2 for $k(e_{aq}^- + S)[S] < 10^9$ s^{-1}; however, by 10^{10} s^{-1} the effect is significant. The yield of H_2 in H_2O_2 solutions is 0.17 according to both experiment and calculation. This value is also obtained in calculations for NO_3^- solutions if it is assumed that the unimolecular H_2 is unscavengable. The yield of H_2 predicted assuming a scavengable precursor to the unimolecular H_2 is 0.10, which corresponds to 0.09 measured in NO_3^-.

4. Discussion

Stochastic diffusion kinetic calculations using the IRT methodology coupled with electron track structures simulated using cross sections appropriate for liquid water have been used to elucidate the contribution of the precursor of the hydrated electron to the radiation chemical kinetics of water and aqueous solutions. In deaerated water, the conversion of e_{pre}^- to e_{aq}^- takes place on the subpicosecond time scale with the yields of the two species being ∼0.1 and 4.8 at 1 ps. Because of the short lifetime of e_{pre}^-, it does not contribute significantly to the observable intratrack chemistry in the electron radiolysis of water. The importance of e_{pre}^- in determining observable chemistry in the radiolysis of scavenger solutions is determined by the solute in question. When the reaction between the scavenger and e_{aq}^- is fast, as for Cd^{2+}, it is not possible to distinguish between reaction of the scavenger with e_{pre}^- and with e_{aq}^-. Consequently, the effect of e_{pre}^- scavenging is not observable unless the products of the two reactions are different. For less efficient scavengers of e_{aq}^-, such as NO_3^-, the scavenging of e_{pre}^- is distinguishable in concentrated solutions but not in dilute solutions. When the reaction of the scavenger with e_{aq}^- is slow but that with e_{pre}^- is efficient, for instance SeO_4^{2-}, the significance of e_{pre}^- is obvious even in dilute solutions. Comparison of R_{pre} with the effective radius of the scavenger in Table 3 shows that scavenging of e_{pre}^- is generally related to the size of the scavenger species.

The aqueous radiation chemistry of three different electron scavengers, SeO_4^{2-}, NO_3^-, and Cd^{2+}, has been considered in detail. These scavengers were selected as they have similar C_{37} values but very different values for $k(e_{aq}^- + S)$. The predictions of the calculations for NO_3^- and for Cd^{2+} are in good agreement with experimental data, but unfortunately no data is available for SeO_4^{2-}. The total yield of electron scavenging by Cd^{2+} is the same as that predicted for a generic e_{aq}^- scavenger that does not react with e_{pre}^-. The yield of Cd^+ is unaffected by the inclusion of e_{pre}^- in the reaction scheme as the reaction of Cd^{2+} with both types of electrons is rapid, with R_{eff} being larger than the scavenging radius of Cd^{2+} for e_{pre}^-. At high NO_3^- concentrations, the amount of electrons scavenged is larger than predicted for a generic e_{aq}^- scavenger. In this case, the magnitudes of R_{eff} and R_{pre} are similar. For SeO_4^{2-}, the scavenging radius for e_{pre}^- is an order of magnitude larger than R_{eff} and the yield of electrons scavenged is dominated by the reaction ($e_{pre}^- + SeO_4^{2-}$) and is much larger than that predicted for a generic e_{aq}^- scavenger.

Acknowledgment. The research described herein was supported by the Office of Basic Energy Science of the U.S. Department of Energy. This is Contribution NDRL-4043 of the Notre Dame Radiation Laboratory.

References and Notes

(1) Hamill, W. H. *J. Phys. Chem.* **1969**, *73*, 1341−7.

(2) Aldrich, J. E.; Bronskill, M. J.; Wollf, R. K.; Hunt, J. W. *J. Chem. Phys.* **1971**, *55*, 530−9.

(3) Wolff, R. K.; Aldrich, J. E.; Penner, T. L.; Hunt, J. W. *J. Phys. Chem.* **1975**, *79*, 210−9.

(4) Jonah, C. D.; Miller, J. R.; Matheson, M. S. *J. Phys. Chem.* **1977**, *81*, 1618−22.

(5) Hart, E. J.; Anbar, M. *The Hydrated Electron*; Wiley-Interscience: New York, 1970.

(6) Buxton, G. V. *Proc. R. Soc. London* **1972**, *A328*, 9−21.

(7) Fanning, J. E. Evidence for spurs in aqueous radiation chemistry. Ph.D. Thesis, University of Delaware, 1975.

(8) Jonah, C. D.; Hart, E. J.; Matheson, M. S. *J. Phys. Chem.* **1973**, *77*, 1838−43.

(9) Jonah, C. D.; Matheson, M. S.; Miller, J. R.; Hart, E. J. *J. Phys. Chem.* **1976**, *80*, 1267−70.
(10) Sumiyoshi, T.; Tsugaru, K.; Yamada, T.; Katayama, M. *Bull. Chem. Soc. Jpn.* **1985**, *58*, 3073−5.
(11) Pimblott, S. M.; LaVerne, J. A.; Bartels, D. M.; Jonah, C. D. *J. Phys. Chem.* **1996**, *100*, 9412−5.
(12) Pimblott, S. M.; LaVerne, J. A. *J. Phys. Chem.* **1997**, *101*, 5828−38.
(13) Balkas, T. I.; Fendler, J. H.; Schuler, R. H. *J. Phys. Chem.* **1970**, *74*, 4497−4505.
(14) Shiraishi, H.; Katsamura, Y.; Hiroishi, D.; Ishigure, K.; Washio, M. *J. Phys. Chem.* **1988**, *92*, 3011−7.
(15) Yoshida, H.; Bolch, W. E.; Turner, J. E.; Jacobson, K. B. *Radiat. Prot. Dosim.* **1990**, *31*, 67−70.
(16) Schmidt, K. H.; Han, P.; Bartels, D. *J. Phys. Chem.* **1995**, *99*, 10530−9.
(17) LaVerne, J. A.; Pimblott, S. M. *J. Phys. Chem.* **1991**, *95*, 3196−206.
(18) Peled, E.; Czapski, G. *J. Phys. Chem.* **1970**, *74*, 2903−11.
(19) Gauduel, Y.; Pommeret, S.; Migus, A.; Antonetti, A. *J. Phys. Chem.* **1989**, *93*, 3880−2.
(20) Draganic, Z. D.; Draganic, I. G. *J. Phys. Chem.* **1973**, *77*, 2691−3.
(21) Wolff, R. K.; Bronskill, M. J.; Hunt, J. W. *J. Chem. Phys.* **1970**, *53*, 4211−5.
(22) Lam, K. Y.; Hunt, J. W. *Radiat. Phys. Chem.* **1975**, *7*, 317−38.
(23) Schwarz, H. A. *J. Chem. Phys.* **1971**, *55*, 3647−50.
(24) Czapski, G.; Peled, E. *J. Phys. Chem.* **1973**, *77*, 893−7.
(25) Pimblott, S. M.; Green, N. J. B. *Research in Chemical Kinetics*; Compton, R. G., Hancock, G., Eds.; Elsevier: Amsterdam, 1995; Vol. 3, pp 117−174.
(26) Chernovitz, A. C.; Jonah, C. D. *J. Phys. Chem.* **1988**, *92*, 5946−50.
(27) Rice, S. A. *Diffusion-Limited Reactions*; Elsevier: Amsterdam, 1985.
(28) Clifford, P.; Green, N. J. B.; Pilling, M. J. *Chem. Phys. Lett.* **1982**, *91*, 101−8.
(29) Noyes, R. M. *Prog. React. Kinet.* **1961**, *1*, 129−160.
(30) Green, N. J. B.; Pimblott, S. M. *J. Phys. Chem.* **1989**, *93*, 5462−7.
(31) Pimblott, S. M.; Pilling, M. J.; Green, N. J. B. *Radiat. Phys. Chem.* **1991**, *37*, 377−88.
(32) Pimblott, S. M.; Green, N. J. B. *J. Phys. Chem.* **1992**, *96*, 9338−48.
(33) Abramowitz, M.; Stegun, I. A. *Handbook of Mathematical Functions*; Dover: New York, 1970.
(34) Schwarz, H. A. *J. Phys. Chem.* **1969**, *73*, 1928−37.
(35) Burns, W. G.; Sims, H. E.; Goodall, J. A. B. *Radiat. Phys. Chem.* **1984**, *23*, 143−80.
(36) Turner, J. E.; Magee, J. L.; Wright, H. A.; Chatterjee, A.; Hamm, R. N.; Ritchie, R. H. *Radiat. Res.* **1983**, *96*, 437−49.
(37) Turner, J. E.; Hamm, R. N.; Wright, H. A.; Ritchie, R. H.; Magee, J. L.; Chatterjee, A.; Bolch, W. E. *Radiat. Phys. Chem.* **1988**, *32*, 503−10.
(38) Hill, M. A.; Smith, F. A. *Radiat. Phys. Chem.* **1994**, *43*, 265−280.
(39) Green, N. J. B.; Pilling, M. J.; Pimblott, S. M.; Clifford, P. *J. Phys. Chem.* **1990**, *94*, 251−8.
(40) Paretzke, H. G.; Turner, J. E.; Hamm, R. N.; Wright, H. A.; Ritchie, R. H. *J. Chem. Phys.* **1986**, *84*, 3182−8.
(41) Pimblott, S. M.; LaVerne, J. A.; Mozumder, A. *J. Phys. Chem.* **1996**, *100*, 8595−8606.
(42) LaVerne, J. A.; Pimblott, S. M. *J. Phys. Chem.* **1997**, *101*, 4504−10.
(43) Clifford, P.; Green, N. J. B.; Pilling, M. J. *J. Phys. Chem.* **1982**, *86*, 1318−21.
(44) Clifford, P.; Green, N. J. B.; Pilling, M. J. *J. Phys. Chem.* **1982**, *86*, 1322−7.
(45) LaVerne, J. A.; Mozumder, A. *J. Phys. Chem.* **1986**, *90*, 3242−7.
(46) Pimblott, S. M.; LaVerne, J. A.; Mozumder, A.; Green, N. J. B. *J. Phys. Chem.* **1990**, *94*, 488−495.
(47) Pimblott, S. M.; Mozumder, A. *J. Phys. Chem.* **1991**, *95*, 7291−300.
(48) Clifford, P.; Green, N. J. B.; Oldfield, M. J.; Pilling, M. J.; Pimblott, S. M. *J. Chem. Soc., Faraday Trans.* **1986**, *82*, 2673−89.
(49) Clifford, P.; Green, N. J. B.; Pilling, M. J.; Pimblott, S. M. *J. Phys. Chem.* **1987**, *91*, 4417−22.
(50) Pimblott, S. M. *J. Phys. Chem.* **1992**, *96*, 4485−91.
(51) Buxton, G. V.; Greenstock, C. L.; Helman, W. P.; Ross, A. B. *J. Phys. Chem. Ref. Data* **1988**, *17*, 513−886.
(52) Elliot, A. J.; McCracken, D. R.; Buxton, G. V.; Wood, N. D. *J. Chem. Soc., Faraday Trans.* **1990**, *86*, 1539−47.
(53) Pimblott, S. M.; LaVerne, J. A. *Radiat. Res.*, in press.
(54) Migus, A.; Gauduel, Y.; Martin, J. L.; Antonetti, A. *Phys. Rev. Lett.* **1987**, *58*, 1559−62.
(55) Gauduel, Y.; Pommeret, S.; Antonetti, A. *J. Phys. IV* **1991**, *1*, 127−39.
(56) Reid, R. C.; Sherwood, T. K. *The Properties of Gases and Liquids*; McGraw-Hill: New York, 1958.
(57) Nightingale, E. R. *J. Phys. Chem.* **1959**, *63*, 1381−7.
(58) Allan, J. T. *J. Phys. Chem.* **1964**, *68*, 2697−703.
(59) Barker, G. C.; Fowles, P.; Stringer, B. *Trans. Faraday Soc.* **1970**, *66*, 1509−19.
(60) Hyder, M. L. *J. Phys. Chem.* **1965**, *69*, 1858−65.
(61) Draganic, I. G.; Draganic, Z. D. *J. Phys. Chem.* **1973**, *77*, 765−72.
(62) Buxton, G. V.; Sellers, R. M. *J. Chem. Soc., Faraday Trans. 1* **1975**, *71*, 558−67.
(63) Kelm, M.; Lilie, J.; Henglein, A. *J. Chem. Soc., Faraday Trans. 1* **1975**, *71*, 1132−42.
(64) Wolff, R. K.; Bronskill, M. J.; Aldrich, J. E.; Hunt, J. W. *J. Phys. Chem.* **1973**, *77*, 1350−5.
(65) Pimblott, S. M.; LaVerne, J. A. *J. Phys. Chem.* **1992**, *96*, 746−52.
(66) Ghormley, J. A.; Hochanadel, C. J. *Radiat. Res.* **1955**, *3*, 227.
(67) Kimmel, G. A.; Orlando, T. M.; Vezina, C.; Sanche, L. *J. Chem. Phys.* **1994**, *101*, 3282−6.
(68) Yoshida, H. *Radiat. Res.* **1994**, *137*, 145−51.